ORCA – Online Research @ Cardiff

RSC Advances

Toward anticancer gold-based compounds targeting PARP-1: a new case study

Journal:	*RSC Advances*
Manuscript ID	RA-COM-05-2016-011606.R1
Article Type:	Communication
Date Submitted by the Author:	n/a
Complete List of Authors:	Citta, Anna; University, Scalcon, Valeria; Institute of Neuroscience, Goebel, Peter; Philipps-Universität Marburg, Fachbereich Chemie Bertrand, Benoît; University of East Anglia, Chemistry Wenzel, Margot; Cardiff University Cardiff School of Chemistry, Folda, Alessandra; Università di Padova, Department of Biomedical Sciences Rigobello, Maria Pia; Università di Padova, Dipartimento di Chimica Biologica Meggers, E; Philipps-Universität Marburg, Fachbereich Chemie Casini, Angela; Cardiff University, School of Chemistry
Subject area & keyword:	Bioinorganic chemistry < Chemical biology & medicinal

SCHOLARONE™
Manuscripts

RSC Advances

An international journal to further the chemical sciences

RSC Advances is an international, peer-reviewed, online journal covering all of the chemical sciences, including interdisciplinary fields.

The **criteria for publication** are that the experimental and/or theoretical work must be **high quality**, **well conducted** and **demonstrates a significant advance by adding to the development of the field**.

RSC Advances **2014 Impact Factor* = 3.840**

Thank you for your assistance in evaluating this manuscript.

Guidelines to the referees

Referees have the responsibility to treat the manuscript as confidential. Please be aware of our Ethical Guidelines, which contain full information on the responsibilities of referees and authors, and our Refereeing Procedure and Policy.

It is essential that all research work reported in *RSC Advances* is well-carried out and well-characterised. There should be enough supporting evidence for the claims made in the manuscript. (http://www.rsc.org/journals-books-databases/about-journals/rsc-advances/)

When preparing your report, please:

• comment on the originality and scientific reliability of the work;

• comment on the characterisation of the compounds/materials reported - has this been accurately interpreted and does it support the conclusions of the work; for theoretical works, please comment if enough supporting evidence has been provided;

• state clearly whether you would like to see the article accepted or rejected and give detailed comments (with references, as appropriate) that will both help the Editor to make a decision on the article and the authors to improve it.

Please inform the Editor if:

• there is a conflict of interest

• there is a significant part of the work which you are not able to referee with confidence

• the work, or a significant part of the work, has previously been published

• you believe the work, or a significant part of the work, is currently submitted elsewhere

• the work represents part of an unduly fragmented investigation.

For further information about *RSC Advances,* please visit: www.rsc.org/advances or contact us by email: advances@rsc.org.

*Data based on 2014 Journal Citation Reports®, (Thomson Reuters, 2015).

RSC Advances

Toward anticancer gold-based compounds targeting PARP-1: a new case study

A. Citta,[a,°] V. Scalcon [a,°], P. Göbel,[b] B. Bertrand,[c] M. Wenzel,[c] A. Folda,[a] M.P. Rigobello,[a,*] E. Meggers[b] and A. Casini[c,d,*]

A new gold(III) complex bearing a 2-((2,2'-bipyridin)-5-yl)-1*H*-benzimidazol-4-carboxamide ligand has been synthesized and characterized for its biological properties *in vitro*. In addition to showing promising antiproliferative effects against human cancer cells, the compound potently and selectively inhibits the zinc finger protein PARP-1, with respect to the seleno-enzyme thioredoxin reductase. The results hold promise for the design of novel gold-based anticancer agents disrupting PARP-1 function and to be used in combination therapies.

Gold compounds have recently gained increasing attention in the design of new metal-based anticancer therapeutics,[1-4] including gold(III) complexes with multidentate N-donor or cyclometalating ligands, gold(III) dithiocabamates, gold(I) *N*-heterocyclic (NHC) carbenes, as well as gold(I) alkynyl complexes.[1, 5-7]

Concerning the possible mechanisms of action, early work suggested DNA as the anticancer target for gold complexes. However, later studies showed that actually the inhibition properties of different proteins and enzymes by gold compounds play major roles,[8, 9] whereas interactions with nucleic acids appear to be markedly less relevant, with a few exceptions.[10, 11] For example, thiol-containing enzymes such as gluthathione reductase (GR), gluthathione-S-transferase,[12] cysteine proteases,[13] protein tyrosine phosphatases (PTP), and deubiquitinases (DUBs)[14] were shown to be potently inhibited by gold complexes. Interestingly, recently the water and

glycerol membrane channels termed aquaporins (AQPs) have also been reported to be selectively targeted by certain families of gold(III) complexes,[15-17] which could also been used to unravel the roles of AQPs in cancer cell proliferation.[18]

In this context, among the most studied and recognized targets for gold compounds, the seleno-enzyme thioredoxin reductase (TrxR) has been widely investigated.[19] Human TrxR contains a cysteine-selenocysteine redox pair at the C-terminal active site, and the solvent-accessible selenolate group, arising from enzymatic reduction, constitutes a likely target for "soft" metal ions such as gold. Thus, a number of mono and dinuclear, as well as heteronuclear, gold(I) and gold(III) complexes have shown good correlation between cytotoxic activity and TrxR inhibition properties.[20-29] In addition, mitochondria and the endoplasmic reticulum[30] have been proposed as potential targets for anticancer gold complexes.

Pursuing the search of novel protein targets for anticancer gold compounds, some of us reported on the inhibitory effects of different cytotoxic gold-based complexes with phosphine or bipyridyl ligands, towards the zinc finger (ZF) enzyme poly (adenosine diphosphate (ADP)-ribose) polymerase 1 (PARP-1).[31, 32] Interestingly, Au(III) coordination complexes were among the most efficient in inhibiting PARP-1, at a nM level, followed by Au(I) compounds.

It is worth mentioning that PARPs are considered "the guardian angels" of DNA playing a key role in its repair by detecting DNA strand breaks and catalyzing poly (ADP-ribosylation).[33] Therefore, PARP inhibitors can be used in combination with conventional anticancer agents that act by damaging DNA, such as cytotoxic chemotherapy and radiotherapy, as the PARP inhibitors block the DNA-repair mechanisms that cancer cells use to resist destruction.[34]

Concerning the molecular mechanisms of PARP-1 inhibition by metal complexes, gold ions in either oxidation state 3+ or 1+ are able to induce zinc substitution in ZF models, leading to the formation of the so-called *gold fingers*.[31, 35, 36] Damage of the ZF domain responsible for DNA recognition leads to PARP-1 inhibition.

a. Department of Biomedical Sciences, University of Padova, via Ugo Bassi 58/b, 35131 Padova, Italy.
b. Fachbereich Chemie, Philipps-Universität Marburg, Hans-Meerwein-Strasse 4, 35043 Marburg, Germany.
c. Dept. of Pharmacokinetics, Toxicology and Targeting, Research Institute of Pharmacy, University of Groningen, Antonius Deusinglaan 1, 9713 AV Groningen, The Netherlands.
d. Cardiff School of Chemistry, Cardiff University, Main Building, Park place, Cardiff CF10 3A, United Kingdom.
° Valeria Scalcon and Anna Citta: these authors contributed equally
* Angela Casini and Maria Pia Rigobello: co- corresponding authors
† Footnotes relating to the title and/or authors should appear here.
Electronic Supplementary Information (ESI) available: [details of any supplementary information available should be included here]. See DOI: 10.1039/x0xx00000x

Here, we report on the synthesis of a new gold(III) complex (**2**) bearing the bidentate N-donor ligand (**1**). Notably, the 1H-benzimidazole-4-carboxamide fragment of **1** has been designed as PARP-1 inhibitor acting on the catalytic site of the protein, and not on its ZF DNA binding domain by forming hydrogen bonds between the carboxamide and Ser904 as well as Gly863 within the catalytic site.[37] Ideally, the resulting gold complex should show enhanced properties as PARP-1 targeted agent profiting of the synergic inhibitory effects of both the Au(III) ions and the organic ligand. Thus, **1** and **2** were tested for their PARP-1 inhibition properties *in vitro* directly against the purified enzyme as well as in protein extracts from human cancer cells, against which the compounds also showed antiproliferative properties. Gold finger formation was observed by high-resolution ESI MS upon treatment of the PARP-1 zinc finger model with **2**.

In this context, where multiple protein targets have been identified for cytotoxic gold compounds, it is absolutely necessary to promptly assess selectivity of new families of complexes in order to avoid side-effects, and to construct solid and reliable structure-activity relationships which should orient the design of targeted chemotherapic agents. Therefore, the activity of the compounds as TrxR inhibitors was also tested on both purified enzyme and cell extracts, in comparison to auranofin, the gold(I) anti-arthritic drug with cytotoxic properties *in vitro*,[38] used here as the benchmark inhibitor of TrxR.[39]

To further characterize the mechanisms of anticancer action of the gold(III) complex **2**, the study of its effects on the intracellular redox state was conducted measuring the total and oxidized glutathione content in cancer cells. Moreover, its effects on the mitochondrial membrane potential were also assessed in cancer cells, in comparison to ligand **1**. The obtained results allowed evaluating the selectivity of **2** for PARP-1 vs TrxR, with implications for the design of improved gold-based targeted agents.

Results and Discussion

A practical synthesis of ligand **1** was developed starting from 4-bromo-2,2'-bipyridine through reductive carbonylation[40] providing 2,2'-bipyridine-4-carbaldehyde[41] in 96% yield, followed by condensation with 2,3-diaminobenzamide[42] in 93% yield. Compound **2** was then synthesized adapting procedures used for previously reported Au(III) complexes with bidentate N-donor ligands[43] (Scheme 1) and characterized via different methods as described in the Experimental section (see Supplementary Information Available). Thus, 2-((2,2'-bipyridin)-5-yl)-1*H*-benzimidazol-4-carboxamide (50 mg, 0.16 mmol) in suspension in ethanol (0.5 mL) was reacted with hydrogen tetrachloroaurate (1 eq, 54 mg, 0.16 mmol), also dissolved in ethanol (0.5 mL), in a round-bottom flask equipped with a condenser. The reaction mixture was refluxed overnight during which time a brown precipitate was formed. After cooling down, the precipitate was collected by filtration and washed twice with diethylether (68% yield). The product was characterized by various techniques including ^{1}H and ^{13}C

NMR spectroscopy, mass spectrometry and elemental analysis (see Supplementary Information for details).
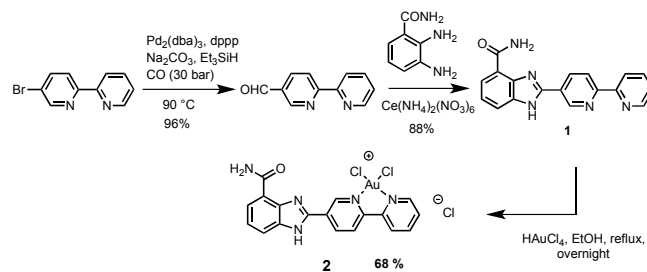
Scheme 1 – Synthesis of ligand **1** and of the related Au(III) complex **2**.

Initially, the stability of the gold(III) complex **2** was evaluated in PBS buffer (pH 7.4) using UV-visible spectrophotometry. The compound exhibits an intense transition in the 300-400 nm range, characteristic of the gold(III) chromophore, that may be straightforwardly assigned as LMCT bands (Fig. S1, supplementary information). Spectral changes are slowly observed with time that might be related to the occurrence of partial hydrolysis processes. In any case, the gold(III) complex is the dominant species in buffered aqueous solutions after several hours incubation.

The stability of **2** toward biologically occurring reducing agent glutathione (GSH) was also evaluated. Results show that GSH, present at a 2:1 molar ratio with respect to **2**, does not markedly affect the evolution of the main LMCT band of the complex with respect to its normal hydrolysis (Fig. S2). However, formation of soluble gold(I) thiolate species as a major product of gold(III) reduction, cannot be excluded.

Afterwards, the antiproliferative properties of the new gold complex **2** and ligand **1** were studied by monitoring their ability to inhibit cell growth using the MTT assay (see Experimental section). Cytotoxic activity of the compounds was determined after exposing for 72 h the human ovarian cancer A2780 cell line, and its cisplatin resistant variant (A2780cisR), the human ovarian cancer SKOV3 cell line, as well as the human non-small cell lung carcinoma A549 line, in comparison to cisplatin and auranofin (AF). The results are summarized in Table 1. The IC$_{50}$ values of **2** towards all tested cell lines are lower in comparison to the free ligand **1**. This may implicate that the gold(III) center plays an important role in the still unknown mechanism(s) of cytotoxic action. The IC$_{50}$ values towards the cisplatin resistant A2780cisR cell line is for **1** comparable to cisplatin, but **2** is markedly more effective. This observation support the idea that in general gold(III) complexes do not have the same mechanism of action as cisplatin, as discussed in the introduction. Both **1** and **2** are poorly toxic against the A549 cell. The greatest difference in IC$_{50}$ value between **1** and **2** is found against the SKOV3 cell line (**2** is ca. 4-fold more potent than **1**). Such discrepancy in the cytotoxic effects may be due to several factors, including different transport mechanisms (uptake and efflux) of complex **2** with respect to ligand **1** in the selected cancer cells, which may lead to decreased intracellular accumulation of **1**. Finally,

AF is certainly the most potent among the tested drugs; however, it is also the most unselective, again demonstrating differences of mechanisms of activity among different families of gold compounds.

Table 1 - IC_{50} values of the Au complexes described in this study against human ovarian carcinoma cell lines SKOV3, cisplatin sensitive (A2780) and resistant (A2780cisR) and lung cancer cells (A549) compared to cisplatin and auranofin (AF).

	IC_{50} (μM)[a]			
Compound	SKOV3	A2780	A2780cisR	A549
1	84.4 ±7.6	9.70±3.06	33.1±5.9	46.7±17.5
2	22.7 ±2.9	4.80±2.35	13.0±2.7	35.0±6.5
AF	1.8± 0.4	1.25± 0.5	1.5± 0.3	2.5± 0.7
cisplatin	13.2 ±3.5	5.2±1.9	35.0±5.9	10.8±2.8

[a] Data are the mean ± SD of at least four experiments.

Compounds **1-2** were then tested against purified PARP-1 using an established protocol.[31] As expected, potent PARP-1 inhibition was observed with both compounds: **1** has an IC_{50} = 5.0 ± 2.1 nM, and **2** has IC_{50}= 6.0 ± 1.3 nM, in the same range as previously reported cytotoxic gold(III) complexes.[31]
Afterwards, PARP-1 activity was evaluated on cell extracts from A2780, A2780cisR and SKOV3 cells. Thus, incubation of protein cell extracts with the compounds for 24 h at room temperature was followed by PARP-1 activity determination. Fig. 1 shows the residual PARP-1 activity in protein extracts treated with the complexes at a fixed concentration (10 μM).
Attractively, both compounds can induce PARP-1 inhibition to a similar extent in A2780 and A2780cisR cell lines, while a marked difference could be detected in the case of SKOV3 cells, where **2** is able to inhibit PARP-1 until ca. 10% of its residual activity. Instead, **1** is practically ineffective on these cells, in line with the scarce anticancer effects observed above. Furthermore, PARP-1 activity was evaluated on protein extracts obtained from SKOV3 cells pre-treated with non-cytotoxic doses of each compound for 48 hours. Afterwards, the protein extracts were collected and analyzed for PARP-1 activity. Preliminary results indicate that only the gold complex **2** (20 μM) was able to induce ca. 70% reduction of PARP-1 activity, while ligand **1** was poorly effective.
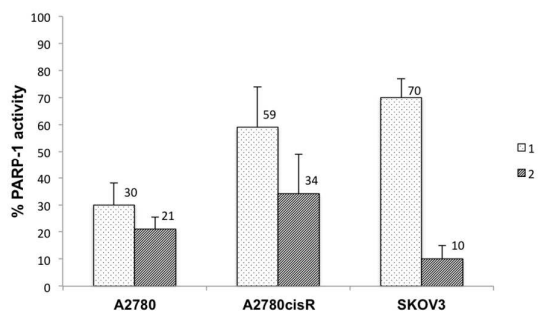

Figure 1 - PARP-1 activity levels in human ovarian cancer cellular extracts. PARP-1 activity was measured in homogenates (50 μg of protein) treated with the compounds

(10 μM) over 24 h at room temperature. Data are the mean ± SD of at least three experiments each performed in triplicate.

In order to assess formation of adducts between the gold complex and the zinc finger domain of PARP-1, a peptide model corresponding to the N-terminal ZF domain sequence of PARP-1 was reacted with **2** and the sample was monitored by high-resolution ESI MS as described in the Experimental section. Figure S3 in the supplementary material shows the broadband mass spectrum of the **2**-ZF adduct. In agreement with previously reported studies on other Au(III) complexes, when **2** was incubated with the ZF domain in a 3 : 1 ratio for 10 min, partial displacement of Zn^{2+} from the ZF by gold ions leads already to formation of the so-called ''gold-finger'' adduct.

Afterwards, to evaluate if the different cytotoxic effects of **2** were related to differences in intracellular Au accumulation, ICP-MS analysis of cell extracts out of A2780 and SKOV3 cells, pre-treated with the gold compound for 24 h, demonstrated that the cytotoxicity is somehow proportional to the gold uptake, and the strongest antiproliferative effects correspond to higher values of intracellular gold concentration. In fact, the concentration of Au [pmol Au/10^6 cells] measured in A2780 and SKOV3 cells is 1802 ± 209 and 1087 ± 322, respectively. Nevertheless, in spite the reduced accumulation of **2** in SKOV3 cells, the inhibition of PARP-1 activity is more pronounced than in the case of A2780 cells (Fig.1).

Since TrxR is also a potential target for gold complexes, *in vitro* inhibition of purified rat TrxR by the two compounds was studied using established protocols as described in the Experimental section. The results are summarized in Table 2 and Figure S4. Complex **2** inhibits cytosolic thioredoxin reductases (TrxR1) in the same range as auranofin (IC_{50} = 14.32 ± 1.62 nM vs IC_{50} = 6.88 ± 1.25 nM, respectively). Conversely, ligand **1** is completely ineffective, as expected since it is deprived of the Au(III) centre able to bind the selenol groups (Figure S1, supplementary information). Further studies demonstrated that **2** is also able to inhibit the TrxR closely related, but selenium-free, enzyme glutathione reductase (GR) with IC_{50} = 0.40 ± 0.06 μM, about 28-fold less efficiently than in the case of TrxR (Table 2).

Afterwards, the effect of compounds on TrxR and GR activities was evaluated in cell lysates. For this purpose, SKOV3 cells where the two compounds showed markedly different cytotoxic effects, were pre-treated for 48 h with 20 and 40 μM of **1** and **2**, respectively. The obtained results show that **1** does not affect enzymes activities, while **2**, causes ca. 50% TrxR inhibition and a slight decrease of GR activity at 40 μM (Fig. 2). In addition, similar experiments were conducted in the A2780 cells, and the obtained results showed no statistically significant inhibition of TrxR at the tested compounds' concentrations (Figure S5). Notably, these latter results further corroborate the hypothesis of alternative pharmacological targets for the reported compounds.

Overall, the obtained results on both PARP-1 and TrxR activities, indicate that the cytotoxic gold complex **2** may operate via inhibition of PARP-1, whereas TrxR is only moderately affected. Concerning the observed differences in PARP-1 inhibition by **1** and **2**, it may be suggested that the ligand is not so selective for binding to PARP-1 as the gold complex **2**, once in the presence of other intracellular components. Nevertheless, in terms of the overall cytotoxic potency, differences in the uptake mechanisms and cellular accumulation between the two compounds should also be taken into account.

Table 2 IC_{50} values of the inhibition of TrxR1 and GR on the isolated enzymes.

	IC_{50} (nM)	
Complexes	TrxR1	GR
1	>100	>10000
2	14.32 ± 1.62	400 ± 60
AF	6.88 ± 1.25	>10000

The glutathione redox pair (GSH/GSSG) is another fundamental component of the cell redox regulation in cisplatin resistant cells.[44] Therefore, our study continued with the analysis of total glutathione content (reduced + oxidized) and of the GSH/GSSG ratio in SKOV3, after treatment with the two compounds for 48 h in comparison to AF. The obtained results are shown in Figure S6 in the Supplementary material available. It can be observed that for all tested compounds no statistically significant variation of the total GSH content, as well as of the GSH/GSSG ratio occur, again made exception for **2**, which causes a slight increase of GSSG content at 40 μM, in accordance with the compound's above-mentioned inhibition effect of glutathione reductase. This behavior suggests that GSH does not particularly influence the cytotoxic potency of the gold complex, as for cisplatin in the case of certain resistant cancer cells.
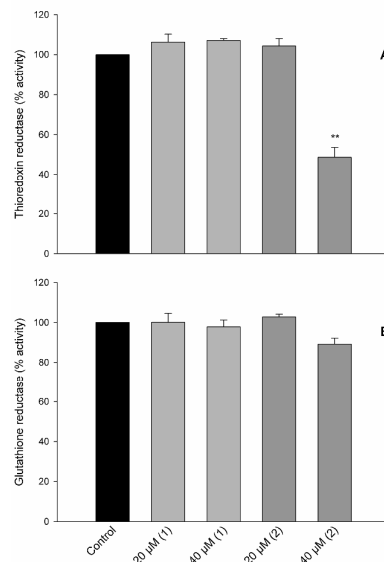

Figure 2 - Effect of the compounds **1** and **2** on thioredoxin reductase and glutathione reductase activities in cell lysates. SKOV3 cells were treated for 48 h with 20 and 40 μM of **1** and **2**, respectively. *= p<0.01

Mitochondrial membrane potential (MMP), a consequence of the electrochemical proton gradient maintained for the purpose of ATP synthesis, is an important indicator of functional mitochondria. Previously reported studies showed that gold(III) complexes are able to determine the decrease of MMP depending on the ligands. As an example, gold(III) Porphyrin **1a** induced apoptosis by mitochondrial death pathways related to reactive oxygen species.[45] Similarly, gold(III)-dithiocarbamato derivatives were shown to alter mitochondrial parameters, such as causing a drop of the mitochondrial membrane potential (MMP).[46]

MMP evaluation was conducted monitoring the fluorescence of tetramethylrhodamine methyl esters (TMRM) according to established protocols (see Experimental for details). Thus, it was possible to determine if the complexes are able to induce a quick drop in mitochondrial membrane potential ($\Delta\psi_m$), detectable as a decline in the fluorescence intensity of TMRM.[47]

Therefore, MMP of SKOV3 cells treated for 18 h with compounds **1** and **2** was measured by cytofluorometric analysis in comparison to auranofin (AF) and CCCP (Fig. 3). Cells were incubated with 25 nM TMRM for 20 min and then analyzed by flow cytometry utilizing an argon laser at 585 nm, as described in the Experimental section.
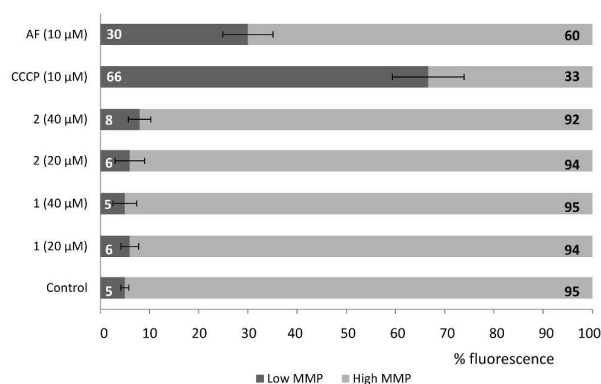
Figure 3 - Percentage of cells with a low and high mitochondrial membrane potential. Mitochondrial membrane potential of SKOV3 cells treated for 18 h with compounds **1** and **2** was measured by a cytofluorometric analysis. Cells were incubated with 25 nM TMRM for 20 min and then analyzed by flow cytometry utilizing an argon laser at 585 nm. Bars represent mean percentages ± S.D. (n=3) of SKOV3 cells whose mitochondria maintained a high (gray) or low (dark gray) TMRM fluorescence, that correspond to their mitochondrial membrane potential.

From the obtained results it has been possible to determine that, at variance with AF and the classical uncoupling agent CCCP (Carbonyl cyanide m-chlorophenyl hydrazone), both complexes **1** and **2** do not affect the MMP values with respect to the controls, as it has instead been reported for gold(III) porphyrins and dithiocarbamato complexes.

Finally, since overexpression of PARP in cancer cells has been linked to drug resistance and PARP-1 inhibition has been shown to sensitize tumor cells to chemotherapeutic agents including platinum compounds, we decided to evaluate the cytotoxic effect of cisplatin administered in combination with different concentrations of **2**. Initial data were obtained for 72 h co-administration of cisplatin (7.5 μM) and **2** at different concentrations (10-20-30 μM) in SKOV3 cells (see experimental for details). In Table S1 (supplementary material) a comparison of the predicted survival rates (defined as the expected cell viability if the combined activities of the compounds are additive) and the experimentally determined values (the observed viabilities) is reported. Unfortunately, the observed survival rates for the combinations of **2** with cisplatin are similar to those predicted on the basis of an additive effect, ruling out the synergism. Further studies will be necessary to investigate possible synergic effects in different cancer cell types and to validate the possibility of using **2** in combination therapy.

Conclusions

We have reported here on the potent PARP-1 inhibition properties of a new cytotoxic gold(III) complex with a bidentate N-donor ligand. A series of biological and biochemical assays has shown that the compound targets preferentially PARP-1 with respect to the seleno-enzyme thioredoxin reductase, and in doing so it is more effective than the free ligand. The absence of effects of the gold(III)

compound on both MMP and intracellular glutathione redox state demonstrate that different mechanisms of action are in place for different families of gold-based cytotoxic agents, which holds promise for the design of targeted anticancer metallodrugs.

Notably, inhibition of PARP potentiates the activity of DNA-damaging agents, such as alkylators, platinum compounds, topoisomerase inhibitors, and radiation in *in vitro* and *in vivo* models. Thus, clinical development to date has focused on PARP inhibitors potential role in combination with DNA-damaging chemotherapy, where efficacy has been limited by enhanced normal tissue toxicity.

Olaparib, a highly potent PARP inhibitor, has recently been approved for ovarian cancer therapy by the FDA and European commission, in patients with platinum-sensitive, recurrent, high-grade serous ovarian cancer with BRCA1 or BRCA2 mutations.[48]

Within this frame, gold(III) complexes such as **2** may constitute an alternative strategy to PARP-1 inhibition, acting on both the zinc finger DNA binding domain of the protein via gold binding, and on its catalytic domain; therefore, having enhanced efficacy. Further studies are necessary to fully validate this hypothesis and to design compounds with selectivity for PARP-1 with respect to other zinc finger proteins.

Notes and references

‡ Footnotes relating to the main text should appear here. These might include comments relevant to but not central to the matter under discussion, limited experimental and spectral data, and crystallographic data.
§
§§
etc.

1.   B. Bertrand and A. Casini, *Dalton Trans*, 2014, 43, 4209-4219.
2.   L. Messori and A. Casini, *Curr Top Med Chem*, 2011, 11, 2647-2660.
3.   T. Zou, C. T. Lum, C.-N. Lok, J.-J. Zhang and C.-M. Che, *Chem. Soc. Rev.*, 2015, 44, 8786-8801.
4.   M. A. Cinellu, I. Ott and A. Casini, in *Bioorganometallic Chemistry*, Wiley-VCH Verlag GmbH & Co. KGaA, 2014, DOI: 10.1002/9783527673438.ch04, pp. 117-140.
5.   E. M. Nagy, L. Ronconi, C. Nardon and D. Fregona, *Mini-Rev Med Chem*, 2012, 12, 1216-1229.
6.   L. Oehninger, R. Rubbiani and I. Ott, *Dalton Trans.*, 2013, 42, 3269-3284.
7.   A. Meyer, C. P. Bagowski, M. Kokoschka, M. Stefanopoulou, H. Alborzinia, S. Can, D. H. Vlecken, W. S. Sheldrick, S. Wolfl and I. Ott, *Angew Chem Int Ed Engl*, 2012, 51, 8895-8899.

8. A. de Almeida, B. L. Oliveira, J. D. G. Correia, G. Soveral and A. Casini, *Coord. Chem. Rev.*, 2013, 257, 2689-2704.

9. A. Casini, G. Kelter, C. Gabbiani, M. A. Cinellu, G. Minghetti, D. Fregona, H. H. Fiebig and L. Messori, *J. Biol. Inorg. Chem.*, 2009, 14, 1139-1149.

10. B. Bertrand, L. Stefan, M. Pirrotta, D. Monchaud, E. Bodio, P. Richard, P. Le Gendre, E. Warmerdam, M. H. de Jager, G. M. Groothuis, M. Picquet and A. Casini, *Inorg Chem*, 2014, 53, 2296-2303.

11. C. Bazzicalupi, M. Ferraroni, F. Papi, L. Massai, B. Bertrand, L. Messori, P. Gratteri and A. Casini, *Angew Chem Int Ed Engl*, 2016, 55, 4256-4259.

12. A. De Luca, C. G. Hartinger, P. J. Dyson, M. Lo Bello and A. Casini, *J. Inorg. Biochem.*, 2013, 119, 38-42.

13. S. P. Fricker, *Metallomics*, 2010, 2, 366-377.

14. J.-J. Zhang, K.-M. Ng, C.-N. Lok, R. W.-Y. Sun and C.-M. Che, *Chem. Comm.*, 2013, 49, 5153-5155.

15. A. P. Martins, A. Marrone, A. Ciancetta, A. Galan Cobo, M. Echevarria, T. F. Moura, N. Re, A. Casini and G. Soveral, *Plos One*, 2012, 7, e37435.

16. A. P. Martins, A. Ciancetta, A. de Almeida, A. Marrone, N. Re, G. Soveral and A. Casini, *ChemMedChem*, 2013, 8, 1086-1092.

17. A. Casini and A. de Almeida, in *Aquaporins in Health and Disease*, CRC Press, 2016, doi:10.1201/b19017-19 pp. 297-318.

18. A. Serna, A. Galan-Cobo, C. Rodrigues, I. Sanchez-Gomar, J. J. Toledo-Aral, T. F. Moura, A. Casini, G. Soveral and M. Echevarria, *Journal of Cellular Physiology*, 2014, 229, 1787-1801.

19. A. Bindoli, M. P. Rigobello, G. Scutari, C. Gabbiani, A. Casini and L. Messori, *Coord. Chem. Rev.*, 2009, 253, 1692-1707.

20. E. Vergara, A. Casini, F. Sorrentino, O. Zava, E. Cerrada, M. P. Rigobello, A. Bindoli, M. Laguna and P. J. Dyson, *ChemMedChem*, 2010, 5, 96-102.

21. J. L. Hickey, R. A. Ruhayel, P. J. Barnard, M. V. Baker, S. J. Berners-Price and A. Filipovska, *J. Am. Chem. Soc.*, 2008, 130, 12570-12571.

22. M. P. Rigobello, L. Messori, G. Marcon, M. A. Cinellu, M. Bragadin, A. Folda, G. Scutari and A. Bindoli, *J. Inorg. Biochem.*, 2004, 98, 1634-1641.

23. C. Gabbiani, G. Mastrobuoni, F. Sorrentino, B. Dani, M. P. Rigobello, A. Bindoli, M. A. Cinellu, G. Pieraccini, L. Messori and A. Casini, *MedChemComm*, 2011, 2, 50-54.

24. R. Rubbiani, L. Salassa, A. de Almeida, A. Casini and I. Ott, *ChemMedChem*, 2014, 9, 1205-1210.

25. E. Schuh, C. Pfluger, A. Citta, A. Folda, M. P. Rigobello, A. Bindoli, A. Casini and F. Mohr, *J. Med. Chem.*, 2012, 55, 5518-5528.

26. A. Citta, E. Schuh, F. Mohr, A. Folda, M. L. Massimino, A. Bindoli, A. Casini and M. P. Rigobello, *Metallomics*, 2013, DOI: 10.1039/c3mt20260g, 1006-1015.

27. B. Bertrand, A. Citta, I. L. Franken, M. Picquet, A. Folda, V. Scalcon, M. P. Rigobello, P. Le Gendre, A. Casini and E. Bodio, *JBIC*, 2015, 20, 1005-1020.

28. N. Lease, V. Vasilevski, M. Carreira, A. de Almeida, M. Sanaú, P. Hirva, A. Casini and M. Contel, *J. Med. Chem.*, 2013, 56, 5806-5818.

29. K. Yan, C. N. Lok, K. Bierla and C. M. Che, *Chem Commun.*, 2010, 46, 7691-7693.

30. J. J. Zhang, R. W. Y. Sun and C. M. Che, *Chem. Comm.*, 2012, 48, 3388-3390.

31. F. Mendes, M. Groessl, A. A. Nazarov, Y. O. Tsybin, G. Sava, I. Santos, P. J. Dyson and A. Casini, *J. Med. Chem.*, 2011, 54, 2196-2206.

32. M. Serratrice, F. Edafe, F. Mendes, R. Scopelliti, S. M. Zakeeruddin, M. Gratzel, I. Santos, M. A. Cinellu and A. Casini, *Dalton Trans.*, 2012, 41, 3287-3293.

33. V. Schreiber, F. Dantzer, J. C. Ame and G. de Murcia, *Nat Rev Mol Cell Bio*, 2006, 7, 517-528.

34. K. Ratnam and J. A. Low, *Clin Cancer Res*, 2007, 13, 1383-1388.

35. U. A. Laskay, C. Garino, Y. O. Tsybin, L. Salassa and A. Casini, *Chem Commun (Camb)*, 2015, 51, 1612-1615.

36. A. Jacques, C. Lebrun, A. Casini, I. Kieffer, O. Proux, J. M. Latour and O. Seneque, *Inorg Chem*, 2015, 54, 4104-4113.

37. T. D. Penning, G.-D. Zhu, J. Gong, S. Thomas, V. B. Gandhi, X. Liu, Y. Shi, V. Klinghofer, E. F. Johnson, C. H. Park, E. H. Fry, C. K. Donawho, D. J. Frost, F. G. Buchanan, G. T. Bukofzer, L. E. Rodriguez, V. Bontcheva-Diaz, J. J. Bouska, D. J. Osterling, A. M. Olson, K. C. Marsh, Y. Luo and V. L. Giranda, *J. Med. Chem.*, 2010, 53, 3142-3153.

38. T. M. Simon, D. H. Kunishima, G. J. Vibert and A. Lorber, *Cancer Res*, 1981, 41, 94-97.

39. M. P. Rigobello, G. Scutari, A. Folda and A. Bindoli, *Biochem. Pharmacol.*, 2004, 67, 689-696.

40. L. Ashfield and C. F. J. Barnard, *Org Process Res Dev*, 2007, 11, 39-43.

41. J. Polin, E. Schmohel and V. Balzani, *Synthesis*, 1998, 1998, 321-324.

42. K. L. Arienti, A. Brunmark, F. U. Axe, K. McClure, A. Lee, J. Blevitt, D. K. Neff, L. Huang, S. Crawford, C. R. Pandit, L. Karlsson and J. G. Breitenbucher, *J. Med. Chem.*, 2005, 48, 1873-1885.

43. A. Casini, M. C. Diawara, R. Scopelliti, S. M. Zakeeruddin, M. Gratzel and P. J. Dyson, *Dalton Trans.*, 2010, 39, 2239-2245.

44. S. Okuno, H. Sato, K. Kuriyama-Matsumura, M. Tamba, H. Wang, S. Sohda, H. Hamada, H. Yoshikawa, T. Kondo and S. Bannai, *British journal of cancer*, 2003, 88, 951-956.

45. Y. Wang, He, Q.Y., Sun, R.W., Che, C.M., Chiu, J.F., *Cancer Res*, 2005, 65, 11553-11564.

46. D. Saggioro, M. P. Rigobello, L. Paloschi, A. Folda, S. A. Moggach, S. Parsons, L. Ronconi, D. Fregona and A. Bindoli, *Chem. Biol.*, 2007, 14, 1128-1139.

47. A. Folda, V. Scalcon, M. Ghazzali, M. H. Jaafar, R. A. Khan, A. Casini, A. Citta, A. Bindoli, M. P. Rigobello, K. Al-Farhan, A. Alsalme and J. Reedijk, *J Inorg Biochem*, 2015, 153, 346-354.

48. C. J. Lord, A. N. Tutt and A. Ashworth, *Annu Rev Med*, 2015, 66, 455-470.

RSC Advances

Supplementary information

Toward anticancer gold-based compounds targeting PARP-1: a new case study

A. Citta,[a,°] V. Scalcon [a,°], P. Göbel,[b] B. Bertrand,[c] M. Wenzel,[c] A. Folda,[a] M.P. Rigobello,[a,*] E. Meggers[b] and A. Casini[c,d,*]

Experimental Section

Synthesis

2,2'-bipyridine-5-carbaldehyde

5-Bromo-2,2'-bipyridine (5.0 g, 21.3 mmol) was dissolved in DMF (29.0 ml). Na_2CO_3 (2.24 g, 21.2 mmol), triethylsilane (7.0 ml, 43.8 mmol) and 1,3-bis(diphenylphosphino)propane (263 mg, 638 µmol) were added. After purging the solution with nitrogen for 10 min, tris(dibenzylideneacetone)dipalladium(0) (390 mg, 426 µmol) was added, the autoclave charged with CO (30 bar), and the reaction stirred at 90 °C for 19 h. After cooling to room temperature and releasing the CO, the black reaction mixture was suspended in water (40 ml) and extracted with Et_2O (4 x 50 ml). The organic phase was concentrated and subjected to silica gel chromatography (*n*-hexane / ethyl acetate 9:1, R_f = 0.31) to provide 2,2'-byridine-5-carbaldehyde (376 g, 20.4 mmol, 96%) as a white solid.

^{1}H-NMR (300 MHz, $CDCl_3$) δ = 10.16 (s, 1H, H11), 9.11 (dd, $^4J_{H10,H8}$ = 2.1 Hz, $^5J_{H10,H7}$ = 0.7 Hz, 1H, H10), 8.72 (ddd, $^3J_{H1,H2}$ = 4.8 Hz, $^4J_{H1,H3}$ = 1.7 Hz, $^5J_{H1,H4}$ = 0.9 Hz, 1H, H1), 8.60 (d, $^3J_{H7,H8}$ = 8.2 Hz, 1H, H7), 8.55–8.47 (m, 1H, H4), 8.27 (dd, $^3J_{H8,H7}$ = 8.2 Hz, $^4J_{H8,H10}$ = 2.2 Hz, 1H, H8), 7.93–7.81 (m, 1H, H3), 7.38 (ddd, $^3J_{H2,H3}$ = 7.5 Hz, $^3J_{H2,H1}$ = 4.8 Hz, $^4J_{H2,H4}$ = 1.2 Hz, 1H, H2). ^{13}C-NMR (75 MHz, $CDCl^3$) δ = 190.7 (C11), 160.8 (C6), 154.9 (C5), 151.8 (C10), 149.6 (C1), 137.3 (C3), 137.0 (C8), 131.2 (C9), 124.9 (C2), 122.4 (C4), 121.4 (C7). FT-IR (Film) = 1697 (CO), 1584, 1553, 1448, 1360, 1249, 1203, 1142, 1084, 1034, 997, 841, 790, 738, 698, 626, 396. HR-MS ESI (+) m/z = 207.0531 (207.0529 calculated for $C_{11}H_8N_2ONa$, $[M + Na]^+$).
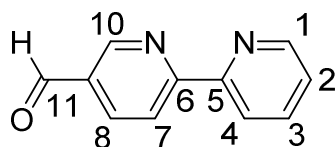
2-((2,2'-bipyridin)-5-yl)-1H-benzimidazol-4-carboxamide

2,2'-bipyridine-5-carbaldehyde (800 mg, 4.34 mmol) and 2,3-diaminobenzamide (722 mg, 4.78 mmol) and Ce(NH4)2(NO396 (360 mg, 0.66 mmol) were carfully mixed. H_2O_2 (30% aqueous solution, 4.0 ml, 39.2 mmol) was added. **Caution:** the reaction is strongly exothermic and proceeds under gas evolution for several minutes. After cooling to room temperature, the brown reaction mixture was suspended in water (100 ml), the water was removed and the solid again washed with water (100 ml). Afterwards, the solid was washed with acetone (50 ml) and the ligand **1** obtained as a brown solid (1.17 g, 3.81 mmol, 88%).

^{1}H-NMR (300 MHz, DMSO-d_6) δ = 13.68 (s, 1H, H1), 9.52 (s, 1H, H19), 9.30 (s, 1H, H8), 8.74 (d, *J* = 5.3 Hz, 2H, H18/H11), 8.59 (d, $^3J_{H12,H11}$ = 8.3 Hz, 1H, H12), 8.48 (d, $^3J_{H15,H16}$ = 7.9 Hz, 1H, H15), 8.09–7.96 (m, 1H, H16), 7.92 (d, $^3J_{H3,H4}$ = 7.5 Hz, 1H, H3), 7.88–7.67 (m, 2H, H5/H1), 7.51 (dd, $^3J_{H17,H16}$ = 6.8 Hz, $^3J_{H17,H18}$ = 5.0 Hz, 1H, H17), 7.40 (t, J = 7.8 Hz, 1H, H4). ^{13}C-NMR (75 MHz, DMSO-d_6) δ = 166.0 (C1), 156.4 (C13 oder 14), 154.4 (C14 oder 13), 149.5 (C18), 149.3 (C9), 147.6 (C19), 141.4 (C6), 137.5 (C16), 135.4 (C11), 135.3 (C10), 125.3 (C7), 124.7 (C17), 123.3 (C4), 122.9 (C3), 122.7 (C2), 120.9 (C15), 120.6 (C12), 115.2 (C5). FT-IR (Film) = 3184, 1662, 1597, 1503, 1458, 1412, 1352, 1316, 1250, 745, 585, 558. HR-MS ESI (+) m/z = 338.1011 (338.1012 calculated for $C_{18}H_{13}N_5ONa$, $[M + Na]^+$). Elemental Analysis, Calculated: C, 68.56; H, 4.16; N, 22.21; Experimental: C, 68.53; H. 4.14; N, 22.24.

1
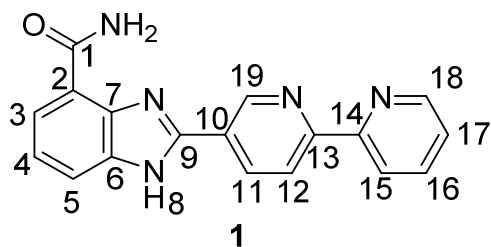
[{2-((2,2'-bipyridin)-5-yl)-1H-benzimidazol-4-carboxamide} AuCl₂]Cl [LAuCl₂]Cl

A round-bottom flask equipped with a condenser, was charged with 2-((2,2'-bipyridin)-5-yl)-1H-benzimidazol-4-carboxamide (50 mg, 0.16 mmol) in suspension in ethanol (0.5 mL). $HAuCl_4.H_2O$ (1 eq, 54 mg, 0.16 mmol) dissolved in ethanol (0.5 mL) was added to the suspension of the ligand. The reaction mixture was refluxed overnight during which time a brown precipitate was formed. After cooling down, the precipitate was collected by filtration and washed twice with diethylether. The product was obtained as a brown powder (67 mg, 68 % yield). ^{1}H NMR (DMSO-d6, 500.13 MHz): 7.44 (broad s, 1 H, H^9), 7.66 (broad s, 1 H, H^2), 7.80 (broad s, 1 H, NH$_2$), 7.85 (d, J_{H-H} = 6.0 Hz, 1 H, H^8), 7.93 (d, J_{H-H} = 6.0 Hz, 1 H, H^{10}), 8.18 (broad s, 1 H, H^3), 8.58 (d, J_{H-H} = 6.0 Hz, 1 H, H^4), 8.63 (d, J_{H-H} = 6.0 Hz, 1 H, H^5), 8.80 (broad s, 1 H, H^1), 8.82 (broad s, 1 H, H^5), 9.07 (broad s, 1 H, NH$_2$), 9.57 (broad s, 1 H, H^7). ^{13}C{^{1}H} NMR (DMSO-d6, 125.76 MHz): 116.7 (s, CH^8), 121.7 (s, CH^5), 122.4 (s, CH^4), 122.7 (s, C^{11}), 123.8 (s, CH$^{9/10}$), 124.1 (s, CH$^{9/10}$), 125.6 (s, C^{12}), 125.9 (s, CH^2), 136.3 (s, C^{15}), 136.9 (s, CH^3, CH^6), 140.2 (s, C^{13}), 148.5 (s, CH^7), 148.6 (s, C^{14}), 149.5 (s, CH^1), 153.1 (s, C$^{16/17}$), 155.0 (s, C$^{16/17}$), 166.7 (s, C=O). (DMSO/MeOH), positive mode exact mass for $[C_{18}H_{13}N_5OAuCl_2]^+$ (582.01572): measured m/z 582.01794 [M-Cl]$^+$. Elemental Analysis, Calculated: C, 34.95; H, 2.12; N, 11.32; Experimental: C, 34.90; H, 2.10; N, 11.36.
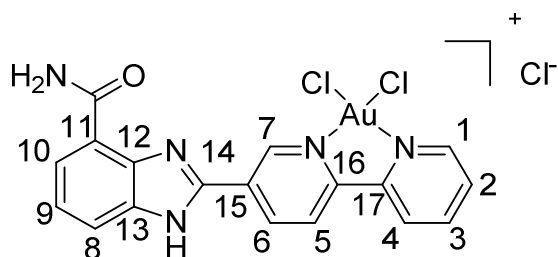
UV-Visible Absorption Spectroscopy

The absorption spectra of the complex **2** in the UV-Visible region were recorded on a Cary 5000 UV-Visible NIR spectrophotometer. The hydrolysis experiments were carried out with a solution of compound **2** 10^{-4} M (from a 10 mM stock solution in DMSO) in PBS buffer (pH 7.4) at room temperature by monitoring the electronic spectra of sample over 24 hours. In another experiment, 2 equivalents of GSH (from a 100 mM stock solution in milliQ water) were added to the same solution (ca. 10^{-4} M complex **2**) in PBS buffer (pH 7.4), and the sample was monitored over 24 h at room temperature.

Cell lines

The human lung cancer A549 and human ovarian cancer cell lines SKOV3, A2780 and A2780cisR (resistant to cisplatin) (obtained from the European Centre of Cell Cultures ECACC, Salisbury, UK) were

cultured respectively in DMEM (Dulbecco's Modified Eagle Medium) or RPMI containing GlutaMaxI supplemented with 10% FBS and 1% penicillin/streptomycin (all from Invitrogen), at 37º C in a humidified atmosphere of 95% of air and 5% of CO_2 (Heraeus, Germany).

Cell growth inhibition studies

Cell viability was evaluated by using a colorimetric method based on the tetrazolium salt MTT ([3-(4,5-dimethylthiazol-2-yl)-2,5-diphenyltetrazolium bromide), which is reduced by viable cells to yield purple formazan crystals. Cells were seeded in 96-well plates at a density of $7-10 \times 10^3$ cells per well (200 µl). After overnight attachment, the medium was replaced by 200 µl of a dilution series of the compounds in the medium, and cells were incubated for further 72 h. Stock solutions of the complexes were prepared in DMSO, made exception for cisplatin which was dissolved in aqueous solution, and Auranofin in EtOH. The percentage of DMSO or ethanol in the culture medium did not exceed 0.2%. At the end of the 72 h incubation period the media was removed and cells were incubated with MTT (0.5 mg/mL in culture medium; 200 µl) for 3-4 h at 37 ºC and 5% CO_2. The purple formazan crystals formed inside the cells were then dissolved in 200 µl of DMSO, and the absorbance was read at 570 nm, using a plate spectrophotometer (Power Wave Xs; Bio-Tek). Each test was performed with at least six replicates and repeated at least 4 times. The IC_{50} value is expressed as percentage of the surviving cells in relation to the control (cells with regular medium).

Additive and Synergistic Cytotoxicity Analysis

The combination index method of Chou and Talaly was used to determine whether the observed interactions between cisplatin and complex 2 were additive or synergistic [Chou, T. C.; Talalay, P. Adv. Enzyme Regulation 1984, 22, 27–55]. If the interaction was additive, the sum of the effects of the two drugs should be equal to the product of their fractional activities. The representative function defined as the expected cell survival rate corresponds to f(u)1,2 = f(u)1 3 f(u)2, where f(u)1 = the fraction unaffected by drug 1, f(u)2 = the fraction unaffected by drug 2, and f(u)1,2 = the fraction unaffected by drugs 1 and 2. The expected and observed cell survival rates obtained from a minimum of six replicates and of at least three repetitions were analyzed by the Student's t test (p): $p < 0.05$ was viewed as significant.

Preparation of cell extracts for PARP-1 activity assays

SKOV3 cells were grown in DMEM GlutaMaxI with 10% FBS (or 3% and 1% when indicated) and incubated with different doses of the compounds. After 48 h, cells were scraped in ice-cold PBS and centrifuged at 10000 g for 10 sec at 4° C. The pellet was re-suspended in 5-10 volumes of lysis buffer (PARP Buffer, Trevigen, Gaithersburg, MD, U.S.A.)) containing protease inhibitor cocktail (Roche, Basel, Switzerland), 0.4 M NaCl, and 1% Triton X-100). After 15 min on ice, lysates were centrifuged at 14000 g for 10 min at 4° C to pellet the cellular debris and the supernatants removed for further use. The total protein content was determined by using the DC Protein Assay Kit (Biorad, Hercules, CA, U.S.A.). Alternatively, cell extracts were incubated with the compounds (different concentrations between 1-40 µM) for 24 hours at room temperature followed by determination of PARP-1 activity as described below.

PARP-1 activity determinations

PARP-1 activity was determined using Trevigen's HT Universal Colorimetric PARP Assay. This assay measures the incorporation of biotinylated poly(ADP-ribose) onto histone proteins in a 96 microtiter strip well format. Either recombinant human PARP-1 (High Specific Activity, purified from *E.coli* containing recombinant plasmid harboring the human PARP gene, supplied with the assay kit) or an aliquot of protein cell extracts (50 µg) was used as the enzyme source. 3-Aminobenzamide (3-AB), provided in the kit, was used as control inhibitor. Purified PARP-1 was incubated with various concentration of

compounds for 1 h at room temperature prior the assay, while cell extracts were either obtained from cancer cells pre-treated with the compounds (48 h), or directly treated with different amounts of gold complexes (24 h) as described above. Two controls were always performed in parallel: a positive activity control for PARP-1 without inhibitors, that provided the 100% activity reference point, and a negative control, without PARP-1 to determine background absorbance. The final reaction mixture (50 μL) was treated with TACS-Sapphire™, a horseradish peroxidase colorimetric substrate, and incubated in the dark for 30 min. Absorbance was read at 630 nm after 30 min. The data corresponds to means of at least three experiments performed in triplicate ± SD.

ESI-MS experiments

The PARP-1 model peptide (GRASCKKCSESIPKDSLRMAIMVQSPMFDGKVPHWYHFSCFWKV) was purchased from Peptide Specialty Laboratories GmbH (Heidelberg, Germany). The apo-zinc-finger peptide was dissolved in milliQ water to a stock solution of 1 mM. The disulphide bonds were reduced using 3 molar equivalents of dithiothreitol (DTT) for 2 hours at room temperature. The complex **2** stock solution (10 mM) was prepared in DMSO and stored at -20 °C. A solution of 150 µM in milliQ water was then freshly prepared. Zn^{2+}-reconstituted peptide-**2** adducts were prepared by diluting 10 µL of the peptide stock solution (1 mM in water) with 200 µL of complex **2** (150 µM) in 1.790 mL of milliQ water. This allowed reaching of a gold compound:peptide ratio of 3:1 in each sample (5 µM peptide + 15 µM **2** complex). After 10 minutes incubation, samples were analysed using a Waters Synapt G2-Si TOF mass spectrometer. The samples were infused directly into the MS at 5 µL/min in ES+ve mode. The source was set up at 3.2 kV with a nitrogen gas flux at a pressure of 6.5 bar (1000 L/h). Data analysis and isotope modelling were performed using the Mass Lynx software provided by Waters at a resolution setting of 31.000.

ICP-MS studies

For the evaluation of the cell uptake, cells were seeded in 6-well plates and grown to approximately 70% confluency and incubated with compound **2** at 70 μM for 24 h. At the end of the incubation period, cells were rinsed cells with 5 mL of PBS, detached by adding 0.4 mL enzyme free cell dissociation solution (Millipore) and collected by centrifugation. Cellular extracts were prepared according to established procedures.[C. Bresson et al, *Metallomics* 2013, 5, 133-143] All samples were analysed for their protein content (to establish the number of cells per sample) prior to ICP-MS determination using a BCA assay (Sigma Aldrich). Samples were digested in ICP-MS grade concentrated hydrochloric acid (Sigma Aldrich) for 3 h at room temperature and filled to a total volume of 8 ml with ultrapure water. Indium was added as an internal standard at a concentration of 0.5 ppb. Determinations of total metal contents were achieved on an Elan DRC II ICP-MS instrument (Perkin Elmer, Waltham, M, U.S.A.). The ICP-MS instrument was tuned daily using a solution provided by the manufacturer containing 1 ppb each of Mg, In, Ce, Ba, Pb and U. External standards were prepared gravimetrically in an identical matrix to the samples (with regard to internal standard and hydrochloric acid) with single element standards obtained from CPI International (Amsterdam, The Netherlands). The results are expressed as mean ± SE of at least three determinations.

Thioredoxin reductase and glutathione reductase inhibition studies in vitro

Cytosolic thioredoxin reductase (TrxR1) was prepared from rat liver according to Luthman and Holmgren.[1] The protein content of isolated enzyme was estimated according to Lowry *et al.*.[2] Thioredoxin reductase activity was measured at 25 °C in 0.2 M Na, K-phosphate buffer (pH 7.4) with 5 mM EDTA and 0.25 mM NADPH in presence of **1** and **2**. Reaction was started by the addition of 1 mM DTNB (DNTB = 5,5'-dithiobis- (2-nitrobenzoic acid Ellman's reagent) and followed spectrophotometrically at 412 nm. Yeast Glutathione reductase activity was measured in 0.2 M Tris-HCl

buffer (pH 8.1), 1 mM EDTA, 0.25 mM NADPH in presence of **1** and **2**. The assay was initiated by the addition of 1mM GSSG and followed spectrophotometrically at 340 nm.

Thioredoxin reductases and glutathione reductase assays in SKOV3 cell lysates

SKOV3 cells (6×10^5) were incubated with **1** and **2** for 48 h with refresh after 24 h. After incubation cells were trypsinized and washed with PBS buffer. Each sample was lysed with a modified RIPA buffer containing 150 mM NaCl, 50 mM Tris-HCl (pH 7.4), 1 mM EDTA, 1% TRITON, 0.1% SDS, 0.5% DOC, 1 mM NaF, 0.1 mM PMSF and an antiprotease cocktail ("Complete" Roche, Mannheim, Germany). After 40 min of incubation at 0 ℃, lysates were centrifuged at 14000 g for 5 min. The supernatants were tested for enzyme activities. Aliquots of lysates (50 μg) were subjected to thioredoxin reductase determination in a final volume of 250 μl of 0.2 M Na, K-phosphate buffer (pH 7.4) with 5 mM EDTA, containing 2 mM DTNB. After 2 min the reaction was started with 0.300 mM NADPH. Glutathione reductase activity (80 μg of cell lysates) was measured in 0.2 M Tris-HCl buffer (pH 8.1), 1 mM EDTA, and 0.25 mM NADPH. The assay was initiated by addition of 1 mM GSSG and followed spectrophotometrically at 340 nm as described above.

Glutathione redox state estimation in SKOV3 cell lysates

SKOV3 cells (5×10^5) in complete medium were incubated for 18 h in presence of **1** and **2**. Cells were trypsinized and washed twice with cold PBS and then lysed and deproteinized with 6% meta-phosphoric acid. After 10 minutes at 4° C, samples were centrifuged and supernatants were neutralized with 15% Na_3PO_4 and assayed for total glutathione.[3] Sample aliquots were derivatized with 2-vinylpyridine in order to block reduced glutathione, and oxidized glutathione was then estimated.[4] Protein concentration was determined by the Lowry *et al.* assay in deproteinized samples washed with 1 ml of ice-cold acetone, centrifuged at 11000 g, dried and then dissolved in 62.5 mM Tris-HCl buffer (pH 8.1) containing 1% SDS.

Determination of mitochondrial membrane potential in cancer cells

Mitochondrial membrane potential of SKOV3 cells was analyzed using flow cytometry. 5×10^5 SKOV3 cells in complete medium were incubated for 18 h with different concentrations of compounds **1** and **2**. The changes of the membrane potential induced by the compounds were estimated with a FACSCanto™ II (Becton Dickinson) flow cytometer with an argon laser at 585 nm, using tetramethylrhodamine (TMRM) as a fluorescent dye.

Figure S1. Hydrolysis profiles of the gold(III) complex **2** dissolved in PBS, pH 7.4, over time at room temperature. Concentration of the complex is 9 x 10^{-5} M.
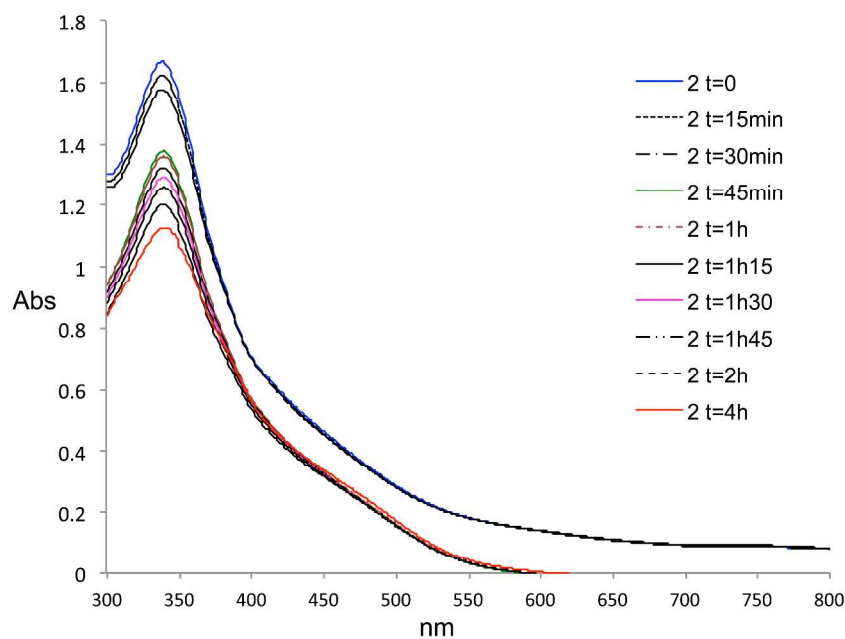

Figure S2. Interaction of the gold(III) complex **2** dissolved in PBS, pH 7.4, with GSH 1:2 over time at room temperature. Concentration of the complex is 1 x 10^{-4} M.
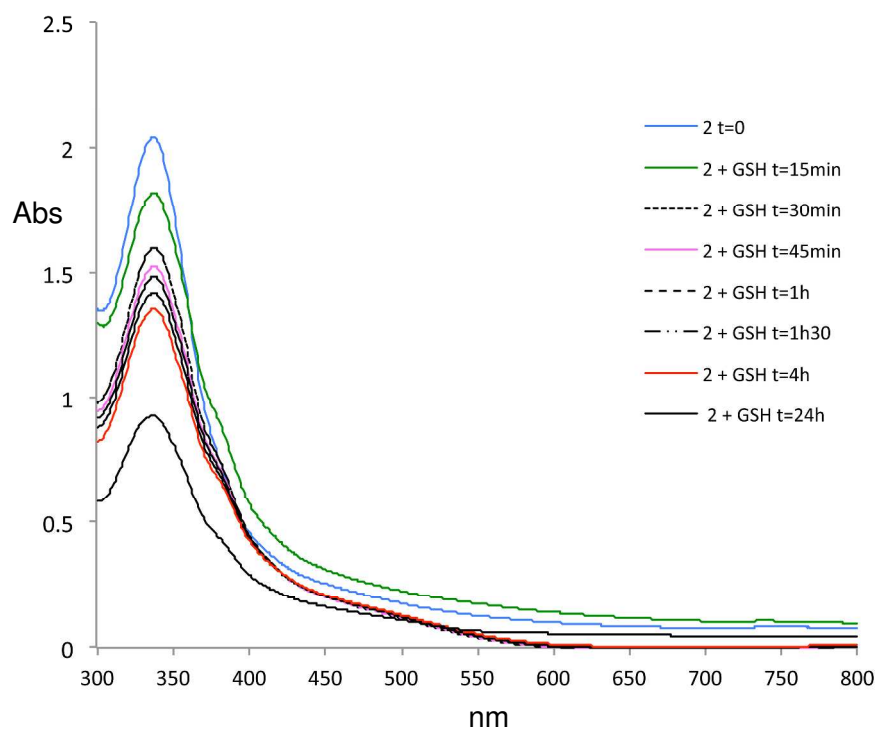
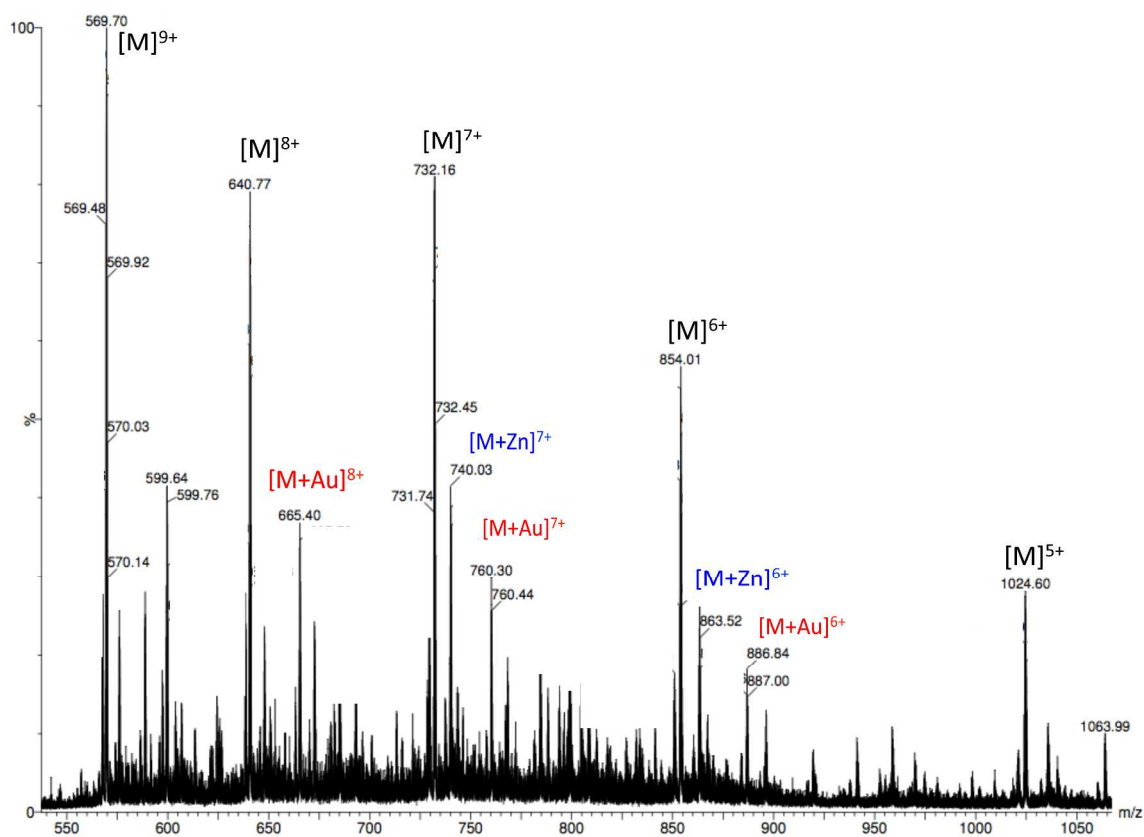**Figure S3**. ESI Orbitrap mass spectrum of the ZF–**2** adduct recorded after 5 min incubation with Zn^{2+} followed by 10 min incubation with **2**.

Figure S4. A: Thioredoxin reductase inhibition by compounds **1, 2** and auranofin (AF). Aliquots of highly purified TrxR1 (60 nM) were incubated in the presence of increasing concentrations of compounds **1, 2** and AF (used as benchmark) and the reaction was followed at 412 nm, as indicated under experimental methods.
B: GR (15 nM) was tested in presence of increasing concentrations of **1**, **2** and AF. NADPH oxidation was followed at 340 nm.
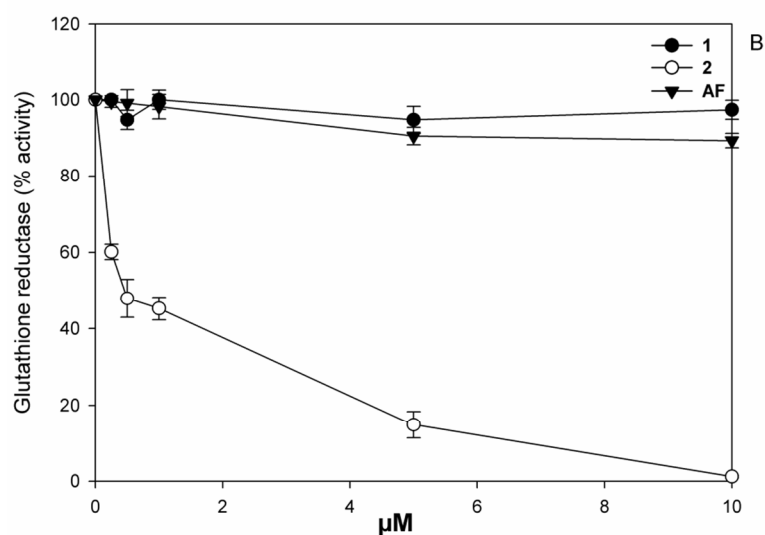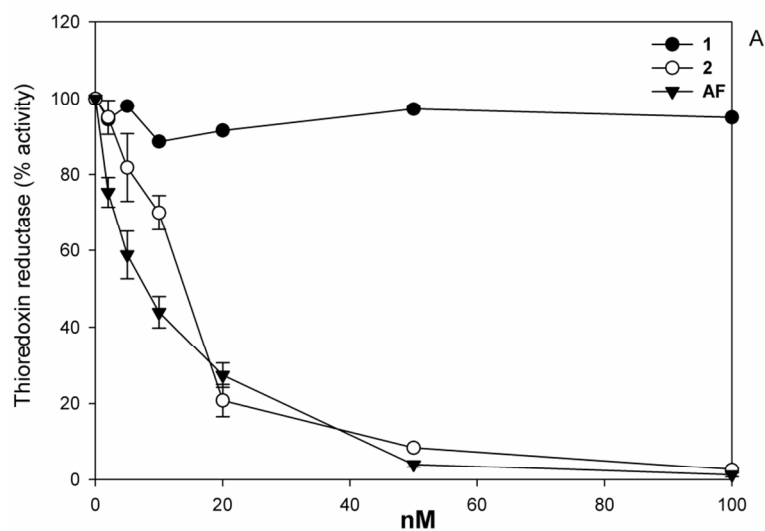
Figure S5. Thioredoxin reductase (A) and glutathione reductase (B) activities in A2780 cell lysates after the treatment with **1** and **2**. 6 x10^5 cells were treated for 48 h with 25 µM **1** and **2**, with a refresh after 24 h.
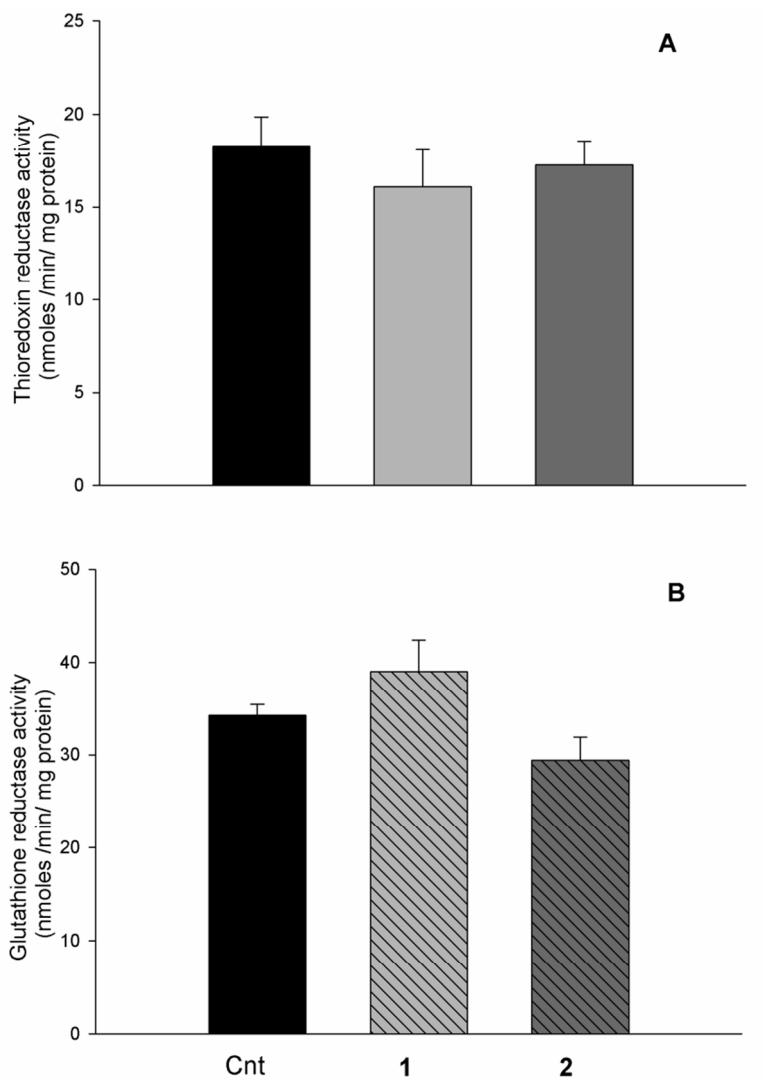
Figure S6. Total glutathione and oxidized glutathione levels in the presence of **1** and **2**.

Total glutathione and oxidized glutathione were determined in SKOV3 cells, after incubation with the indicated concentrations of **1** and **2** for 48 h.

Statistical Analysis. Multiple comparisons were made by one-way analysis of variance followed by the Tukey–Kramer multiple comparison test. *= $p < 0.05$
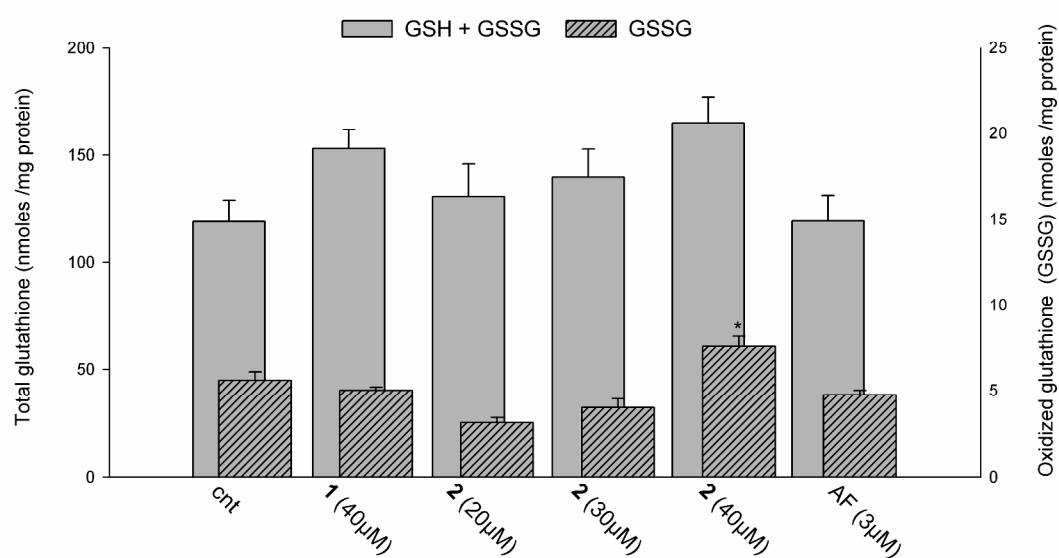
Table S1. Comparison of the Expected Survival Rates (based on an assumption that the Combined Drug Activities are additive) and the Experimentally Determined Values after treating cells for 72 h with cisplatin (7.5 µM) and different concentrations of **2** (10, 20, 30 µM). Calculation of the predicted survival rates is described in the Experimental Section.

	Survival rate	
Drug treatment	*Expected*	*Observed*
Cispt 7.5µM		0.55
Cispt 7.5µM + **2** 10µM	0.445	0.465
Cispt 7.5µM + **2** 20µM	0.24	0.36
Cispt 7.5µM + **2** 30µM	0.165	0.36

References

1.   M. Luthman and A. Holmgren, *Biochem.*, 1982, 21, 6628-6633.
2.   O. H. Lowry, N. J. Rosebrough, A. L. Farr and R. J. Randall, *J. Biol. Chem.*, 1951, 193, 265-275.
3.   F. Tietze, *Anal Biochem*, 1969, 27, 502-522.
4.   M. E. Anderson, *Methods Enzymol*, 1985, 113, 548-555.
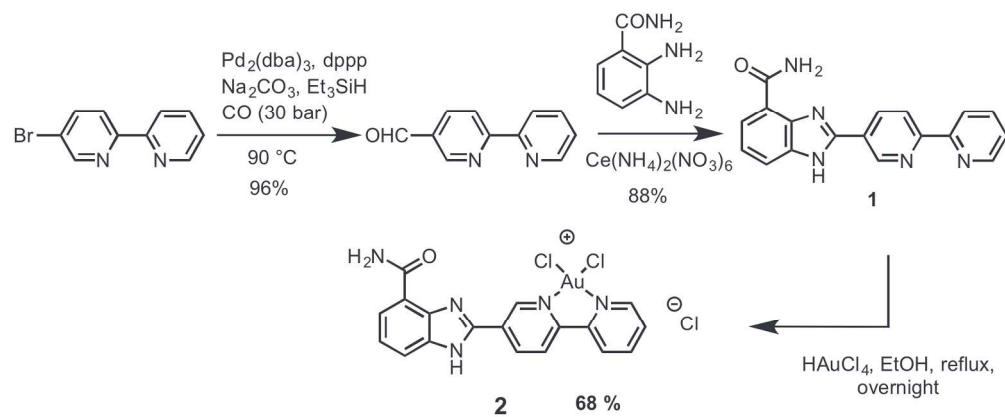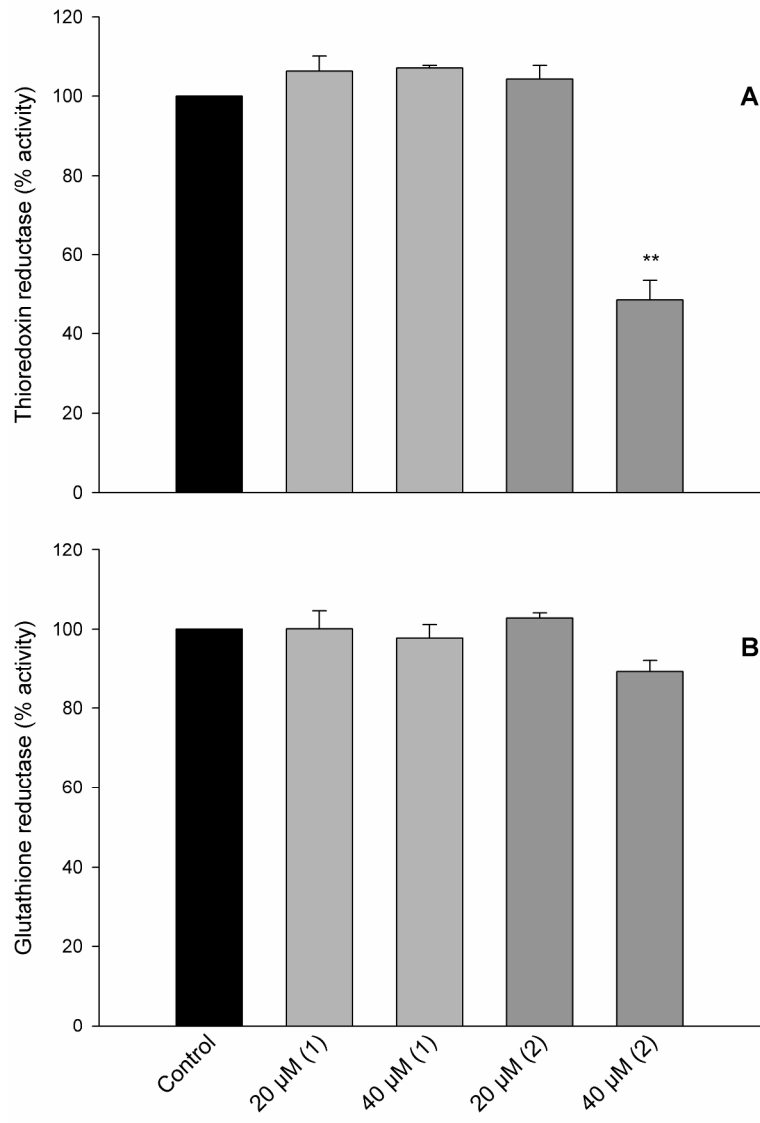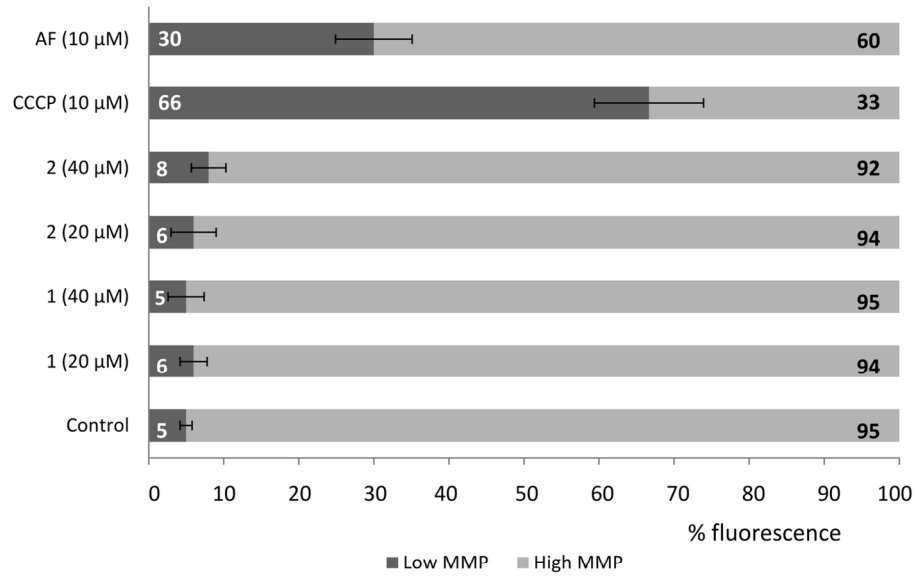
Scheme 1

177x74mm (300 x 300 DPI)

Figure 2

226x328mm (300 x 300 DPI)

Figure 3

129x98mm (300 x 300 DPI)